

# Decay of Cosmic String Loops Due to Particle Radiation

Daiju Matsunami<sup>◦†</sup>, Levon Pogosian<sup>†</sup>, Ayush Saurabh<sup>\*</sup>, Tanmay Vachaspati<sup>\*</sup>

<sup>◦</sup>*Canadian Institute for Theoretical Astrophysics,  
University of Toronto, Toronto, ON M5S 3H8, Canada*

<sup>†</sup>*Physics Department, Simon Fraser University,  
Burnaby, BC V5A 1S6, Canada.*

<sup>\*</sup>*Physics Department, Arizona State University,  
Tempe, AZ 85287, USA.*

Constraints on the tension and the abundance of cosmic strings depend crucially on the rate at which they decay into particles and gravitational radiation. We study the decay of cosmic string loops in the Abelian-Higgs model by performing field theory simulations of loop formation and evolution. We find that our set of string loops emit particle radiation primarily due to kink collisions, and that their decay time due to these losses is proportional to  $L^p$  with  $p \approx 2$  where  $L$  is the loop length. In contrast, the decay time to gravitational radiation scales in proportion to  $L$ , and we conclude that particle emission is the primary energy loss mechanism for loops smaller than a critical length scale, while gravitational losses dominate for larger loops.

High energy particle physics models often predict the existence of cosmic strings [1] and much effort is being devoted to detect these remnants. Detection strategies are mostly focused on the gravitational effects of strings as the string tension can be quite large and, in the current LIGO era, gravitational wave emission provides a promising observational handle on cosmic strings [2]. If cosmic strings decay primarily into gravitational radiation, the tightest constraints on the cosmic string tension,  $\mu$ , comes from the millisecond pulsar timing array [3] and gives the bound  $G\mu \lesssim 10^{-10}$  where  $G$  is Newton's gravitational constant [2, 4]. However, gravitational wave bounds only apply if string loops primarily decay due to gravitational radiation emission. Indeed, field theory simulations of string networks, in contrast to simulations that treat strings as zero-width objects (also called “Nambu-Goto strings”) [5–9], suggest that loops primarily decay into particle radiation [10], potentially leading to a new paradigm for cosmic string evolution in which the gravitational wave bounds do not apply. Thus it is critical to examine particle emission by cosmic string loops and to determine their primary decay mode.

Previous studies of the particle radiation from cosmic strings included analytical estimates [11], some based on effective couplings of zero-width strings to other fields [12, 13], field theory simulations of standing waves, kinks and cusps on long strings [14, 15] and simulations of strings with small oscillations [10, 16]. In this work, for the first time, we directly examine the decay of a single loop of cosmic string to particle radiation in the Abelian-Higgs model by simulating loop formation followed by evolution in full field theory. The focus on a single loop is to be contrasted with the very large field theory simulations of an entire network of strings in an expanding spacetime [10, 17].

Our results are summarized as follows. Cosmic string loops emit particle radiation mainly due to special fea-

tures on the strings known as kinks and cusps [1]. The half-life of a loop due to particle radiation is proportional to  $L^p$ , where  $L$  is the length of the loop and  $p \approx 2$  for the set of loops we have considered. On the other hand, the half-life of a loop due to gravitational wave emission is known to be proportional to  $L$ . Thus, there is a crossover from particle-decay to gravitational-decay roughly given by  $L_* \sim w/G\mu$  where  $w \sim \mu^{-1/2}$  is the width of the string. For  $L < L_*$ , loops decay by particle emission, while for  $L > L_*$  gravitational emission dominates. We will discuss caveats and the implications of this result in more detail below, where we also discuss values of  $p$  that might arise for loops other than those we have directly simulated.

We consider the Abelian-Higgs field theory with a complex scalar field,  $\phi = \phi_1 + i\phi_2$ , and a U(1) gauge field,  $A_\mu$ . We work in the temporal gauge,  $A_0 = 0$ , and the field equations of motion are

$$\partial_t^2 \phi_a = \nabla^2 \phi_a - e^2 A_i A_i \phi_a - 2e\epsilon_{ab} \partial_i \phi_b A_i - e\epsilon_{ab} \phi_b \Gamma - \lambda(\phi_b \phi_b - \eta^2) \phi_a \quad (1)$$

$$\partial_t F_{0i} = \nabla^2 A_i - \partial_i \Gamma + e(\epsilon_{ab} \phi_a \partial_i \phi_b + e A_i \phi_a \phi_a) \quad (2)$$

$$\partial_t \Gamma = \partial_i F_{0i} - g_p^2 [\partial_i F_{0i} + e\epsilon_{ab} \phi_a \partial_i \phi_b], \quad (3)$$

where  $a = 1, 2$ ,  $\epsilon_{ab}$  is the Levi-Civita tensor with  $\epsilon_{12} = 1$ ,  $F_{0i} = \partial_t A_i$  in the temporal gauge,  $\lambda$  and  $e$  are coupling constants,  $\Gamma \equiv \partial_i A_i$ , and  $g_p^2$  is a parameter introduced for numerical stability [18].

Topological solutions in the Abelian-Higgs model were found in Ref. [19]. The solution for a straight string along the  $z$ -axis is,

$$\phi = \eta f(r) e^{i\theta}, \quad A_i = v(r) \epsilon_{ij} \frac{x^j}{r^2} \quad (i, j = 1, 2) \quad (4)$$

where  $r = \sqrt{x^2 + y^2}$ ,  $\theta = \tan^{-1}(y/x)$ , and  $f(r)$  and  $v(r)$  are string profile functions that vanish at the origin and asymptote to 1, respectively. The string energy per unit

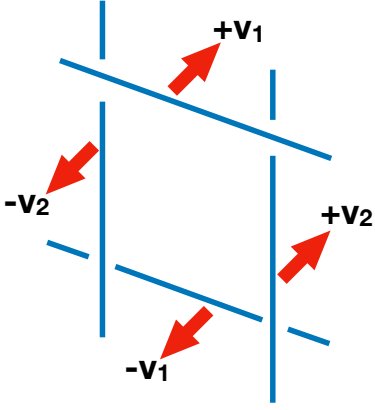


FIG. 1: Schematic representation of the initial configuration. Four straight strings are set up with velocities as shown. The strings intersect and reconnect to produce a central loop and also a second “outer” loop because of periodic boundary conditions. These loops then oscillate and shrink without interacting with each other. By choosing the spacing of the initial strings, we can produce loops of different sizes.

length (also its tension) is given by  $\mu = \pi\eta^2 F(\beta)$  where  $\beta \equiv 2\lambda/e^2$  and  $F$  is a numerically determined function. In the current work we will only consider  $\beta = 1$ . Since  $F(1) = 1$ ,  $\mu = \pi\eta^2$ . Also the scalar mass,  $m_S = \sqrt{2}\lambda\eta$ , equals the vector mass,  $m_V = e\eta$ , in this so-called BPS (Bogomol’nyi-Prasad-Sommerfield limit [20, 21]) case.

Our aim is to produce a loop as might be produced in a cosmological setting and then to evolve it. For this purpose, we set up initial conditions with four straight strings that are moving with velocities  $\pm\mathbf{v}_1$  and  $\pm\mathbf{v}_2$  as shown schematically in Fig. 1. The four strings then collide to form a loop with a stationary center of mass and a non-zero angular momentum. The latter is essential to prevent the loop from simply collapsing to a double line. The preparation of this initial configuration is reasonably involved, since the string solution of Eq. (4) needs to be oriented along different directions, then boosted to a suitable velocity, gauge transformed to stay within the temporal gauge, and finally all the four string configurations have to be patched together in a simulation box with periodic boundaries. The relevant details are provided in the Supplemental Material section.

Cosmological strings are expected to be mildly relativistic and we choose  $|\mathbf{v}_1| = 0.6$  and  $|\mathbf{v}_2| = 0.33$ . The directions are taken to be  $(\hat{v}_1)_x = 0.4$ ,  $(\hat{v}_1)_y = \sqrt{1 - 0.4^2} \approx 0.92$  for the two strings oriented along the  $z$ -axis and  $(\hat{v}_2)_z = 0.4$ ,  $(\hat{v}_2)_y \approx 0.92$  for the strings along the  $x$ -axis. The strings velocities are approximately aligned along the  $y$ -axis, but not exactly, to avoid overly symmetrical loops that tend to pass through a double line configuration and collapse prematurely. We have experimented with a wide range of initial velocities and our main conclusions are independent of the particular choices of these

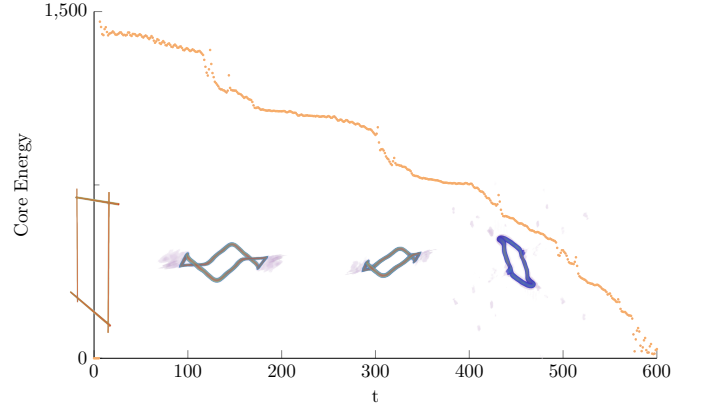


FIG. 2: Energy of a loop with the initial size of 390 lattice spacings plotted vs time. Overlaid on the plot are snapshots of the loop as it goes through phases of rapid radiation discharge due to smoothening of kinks. The animation showing the evolution of this loop can be found at [23].

parameters.

Once we have set up the initial conditions for fields  $\phi$ ,  $A_\mu$  we evolve them using the discretized version of Eqs. (1)-(3). We use the explicit Crank-Nicholson algorithm with two iterations for the evolution [22] and employ periodic boundary conditions. For the numerical parameter we use  $g_p^2 = 0.75$  and we vary the lattice spacing  $\Delta x$  to study the effects of numerical resolution. We keep the initial string spacing to be a fixed fraction of the simulation box size so that smaller loops run in a smaller box, with less computational cost. We also set  $e = 1$ ,  $\lambda = 1/2$ ,  $\eta = 1$ .

Because of periodic boundary conditions, the reconnection of four strings produces two loops – the central loop in the middle of the box shown in Fig. 1, and an “outer” loop formed from the “fragments” in the corners of the box. The two loops then oscillate and decay without intersecting each other. We track the energy in a loop by summing the energy density in the “core” of the string. The energy density is given by

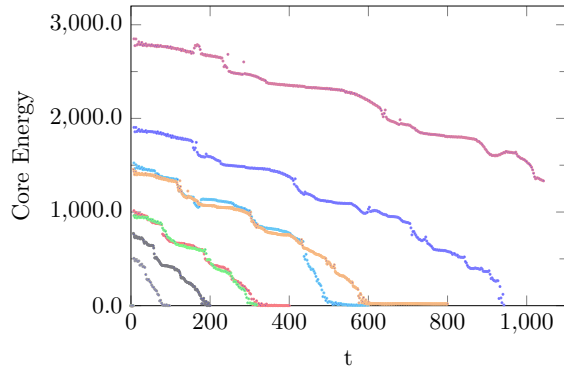
$$\mathcal{E} = \frac{1}{2}|D_0\phi|^2 + \frac{1}{2}|D_i\phi|^2 + \frac{1}{2}(\mathbf{E}^2 + \mathbf{B}^2) + \frac{\lambda}{4}(|\phi|^2 - \eta^2)^2 \quad (5)$$

where  $\mathbf{E}$  and  $\mathbf{B}$  are the electric and magnetic field vectors, respectively, with their components defined as  $E_i = F_{0i}$  and  $B_i = -\frac{1}{2}\epsilon_{ijk}F_{jk}$ . We define the string core to be the cells where the magnitude of the scalar field,  $|\phi|$ , is less than  $0.9\eta$ .

In Fig. 2 we plot the loop energy vs time for a simulation on a  $600^3$  lattice with  $\Delta x = 0.25$ , where the initial size of the loop is 390 lattice spacings. (The animation of the loop evolution can be found at [23].) The plot suggests episodic radiation, with the overlaid snapshots showing the representative “events” leading to drops in the loop energy. Straight strings do not radiate as they correspond to a boosted string solution. The kinks on

Lattice size	Inner loop	Outer loop
$400^3$	140	260
$600^3$	210	390
$800^3$	280	520
$1200^3$	420	780

TABLE I: Loop sizes in lattice units for each of the runs.

FIG. 3: Loop energy vs. time for 8 different loops in 4 separate runs. These runs are with  $\Delta x = 0.25$  resolution.

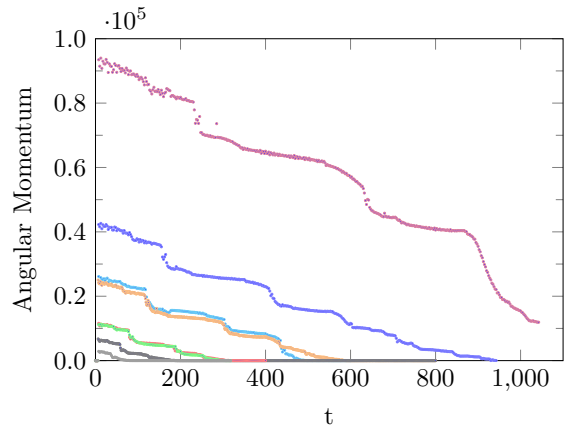
the loop, formed at the intercommutation of the straight strings, also propagate with minimal energy loss. We find that noticeable radiation is produced when kinks collide. Also, as the kinks smooth out, there are episodes of large radiation which may be due to the formation of weak cusps. Particle radiation from cusps has been studied in Ref. [14] where it is found that the energy emission from a cusp leads to the formation of kinks and to weak cusps in subsequent loop oscillations. The pattern of episodic radiation from kink collisions and weak cusps, with relatively minor energy loss in between these events, is common to all loop simulations we have performed.

To obtain a quantitative measure of the scaling of the loop half-life with its size, we have run simulations for 4 different box sizes yielding 8 loops given in Table I. (Two loops from different runs are almost the same length and provide a check on our simulation.) Fig. 3 shows the loop energy versus time for the 8 loops. As the loops evolve, they also shed their angular momentum, defined as

$$L_i \equiv \epsilon_{ijk} \int_{\text{string core}} d^3x x_j \left[ -\frac{1}{2} ((D_0\phi)(D_k\phi)^* + (D_0\phi)^*(D_k\phi)) + \epsilon_{klm} E_l B_m \right]. \quad (6)$$

In Fig. 4 we plot  $|\mathbf{L}|$  vs time and also see episodic decay.

We have run our simulations for a few different values of the lattice spacing,  $\Delta x$ , and found that the results are sensitive to the resolution. For example, as shown in Fig. 5, the total energy in the simulation box over the entire run is conserved only at  $\sim 33\%$  level when  $\Delta x = 0.50$ . Recall that we have set  $\eta = 1$ ,  $e = 1$ ,  $\lambda = 1/2$  and so

FIG. 4: Loop angular momentum vs. time for 8 different loops in 4 separate runs. These runs are with  $\Delta x = 0.25$  resolution.

the string width is  $\sim 1$ . Therefore with  $\Delta x = 0.5$  we only have a few lattice points within the width of the string. The run with  $\Delta x = 0.25$  gives better conservation, to  $\sim 5\%$  level and agrees quite well with the much more computationally expensive run with  $\Delta x = 0.125$ . The choice of  $\Delta x$  makes an important difference in the lifetime of the loop, as is clear from the right panel of Fig. 5. Loops live longer when the simulation resolution is better. By examining animations of the loops we see that the shorter loops live for about one oscillation period while the larger loops survive for several oscillation periods. (There is ambiguity in defining an oscillation period since the length of the loop and hence its oscillation period is changing relatively rapidly during the simulation.)

The longest loop we are able to simulate has energy  $\sim 3 \times 10^3$ , which corresponds to length  $L \sim 10^3 w$  where  $w$  is the width of the string. In cosmology we are interested in loops whose length can be comparable to the cosmic horizon,  $t$ , which is orders of magnitude larger than the thickness of the string, perhaps even by a factor  $\sim 10^{60}$ . So we need to extrapolate our results to larger lengths. For this purpose we calculate the half-life,  $\tau$ , of the loops in our simulations – the time taken for the loop to lose half its initial energy. We normalize this by the half-life of the smallest loop in our simulations,  $\tau_0 = 41.5/\eta$ . In Fig. 6 we plot  $\tau/\tau_0$  versus the initial energy of the loop normalized by the energy of the smallest loop (denoted  $E_0 = 506\eta$ ) on a log-log scale. We find a power law fit,

$$\tau = \tau_0 \left( \frac{E}{E_0} \right)^p = \frac{1.6 \times 10^{-3}}{\eta} (\eta L)^p, \quad p \approx 2 \quad (7)$$

where we have reinserted dimensional factors of  $\eta$ .

The  $L^2$  scaling in (7) can be understood as following from radiation being due to episodes involving a fixed number of features (kinks and weak cusps) on the loop,

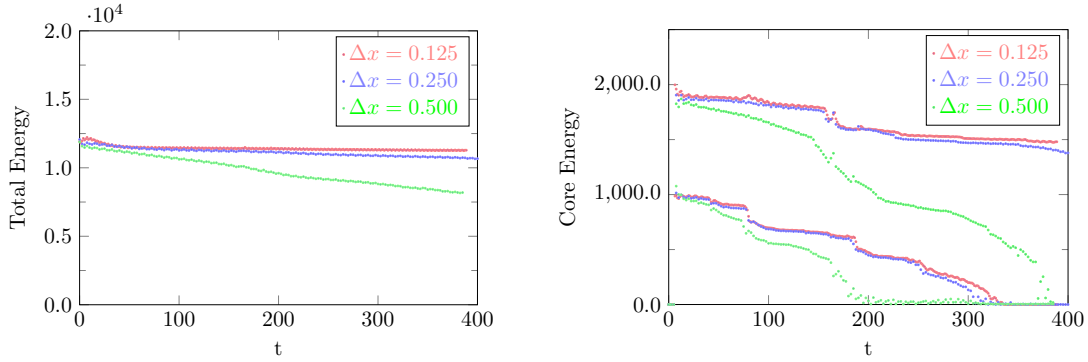


FIG. 5: Comparison of runs with different lattice resolution  $\Delta x = 0.125, 0.25, 0.5$  on lattices of size 800, 400 and 200, respectively, corresponding to a fixed physical lattice length of 100. The left panel shows the total energy in our simulation box and the right panel shows the evolution of the energy in the two loops in the box. The plots show convergence at higher resolution and that  $\Delta x = 0.25$  offers a good compromise between accuracy and speed.

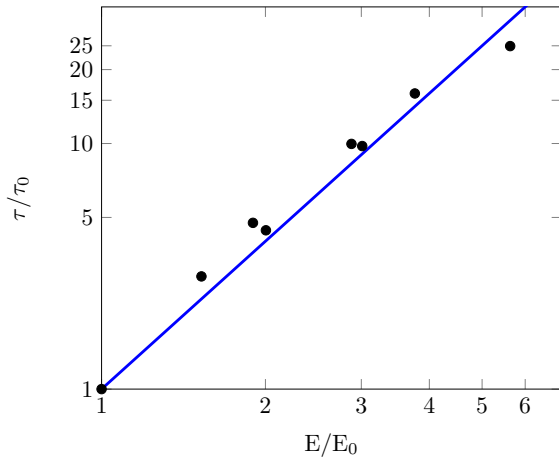


FIG. 6: Log-log plot of the half-life of a loop versus initial energy (proportional to initial length) in the loop. The half-life and energy are normalized by the initial half-life,  $\tau_0$ , and energy,  $E_0$ , of our smallest loop. The straight line fit shows that  $\tau \propto L^2$  where  $L$  is the initial length of the loop.

with the power emitted in a given episode (a kink collision or a weak cusp) being independent of  $L$ . (Note that the size of the steps seen in Fig. 3 is similar for different loops). If  $\nu$  denotes the number of episodes per period and each episode radiates energy  $\epsilon$  on average, the energy lost per unit time is

$$\dot{E} \sim -\frac{\nu\epsilon}{L} \sim -\frac{\mu\nu\epsilon}{E}. \quad (8)$$

Integration of this equation gives a lifetime

$$\tau \sim \frac{E^2}{\mu\nu\epsilon} \sim \frac{\mu L^2}{\nu\epsilon} \quad (9)$$

in agreement with the  $L^2$  scaling in (7).

The particle radiation rate (8) is to be contrasted with  $\dot{E} \sim \nu G\mu^2$  expected due to gravitational wave radiation from  $\nu$  radiation episodes involving kinks and cusps [24–26]. Note that the rate of energy loss to gravitational radiation is not suppressed by a factor of  $L$  as is the case for particle radiation in (8). This is because, for example, a cusp on a loop that is twice as large is also twice as large, and the gravitational energy emitted by a single cusp is proportional to  $L$ . Then the lifetime of the loop due to gravitational radiation is

$$\tau_g \sim \frac{L}{\nu G\mu}. \quad (10)$$

Comparing this to (9) allows us to derive a criterion for when the gravitational radiation is more important than particle radiation, namely, when

$$\tau_g < \tau \Rightarrow L \gtrsim \frac{\epsilon}{G\mu^2} \sim l_P (G\mu)^{-3/2} \quad (11)$$

where we estimate  $\epsilon \sim \sqrt{\mu}$ , *i.e.* the particle energy emitted in an episode is comparable to the energy scale of the string, and  $l_P \sim 10^{-33}$  cm is the Planck length. Note that the number of episodes,  $\nu$ , has canceled out in (11). Therefore even if the number of episodes is larger on larger loops, gravitational radiation still dominates over particle radiation if (11) is satisfied.

With  $L \sim 10^{27}$  cm we find that gravitational radiation is never more important than particle radiation if  $G\mu \lesssim 10^{-40}$  which corresponds to  $\eta \sim 100$  MeV or the QCD scale. Hence particle radiation could be the dominant decay mechanism for strings formed below the QCD scale but the dynamics of cosmic strings formed at such low energy scales is expected to be dominated by friction with the ambient medium [1].

Alternately, we can consider strings close to the current bound on the string tension,  $G\mu \approx 10^{-11}$ . From Eq. (11), particle radiation from such strings will only be

important for loops that are very small,  $L < 10^{-17}$  cm. Most of the radiation from such a network of strings will be in gravitational waves.

We would like to point out some caveats to the above discussion. The first caveat is that the long strings in our initial conditions are straight and smooth. If these strings started out with structure (perhaps as shallow kinks) on them, as has been suggested in Ref. [17], the number of radiative episodes would be larger, and both the particle and gravitational radiation would be larger. This would not change the relative importance of particle and gravitational radiation but it would mean that the loop decays faster. A second caveat is that our loops only contain kinks and no cusps. It is known from Ref. [14] that the radiation loss from a cusp is proportional to  $\sqrt{L}$  and this does not agree with our model where each episode emits radiation that is independent of  $L$ . However, once the cusp radiates, it forms two kinks that then propagate, radiate and smooth out to some extent. In the next oscillation, the cusp is weaker and the energy radiated will not be proportional to  $\sqrt{L}$ , instead it will be proportional to some power of  $L$  smaller than  $1/2$ . Thus with cusps we expect that the effective value of  $p$  will satisfy  $1 < p < 3/2$ , and Eq. (11) will get modified. Even then there will be a critical loop length such that gravitational emission dominates over particle radiation for larger loops. A third caveat is that since our initial strings were straight, there was no radiation while the kinks propagate on the straight segments. If, however, the segments are curved, there will be some radiation even from a propagating kink. This radiation would not be episodic but it would be suppressed by the curvature of the segment, expected to be suppressed by the loop size divided by the cosmic horizon scale.

To summarize, we have studied the formation and evolution of a set of loops of cosmic string in field theory and estimated their lifetimes. On a technical note, we find that the lifetime of our set of loops is very sensitive to the resolution used in their numerical evolution. With insufficient resolution, the loops collapse within one oscillation period. At higher resolution, the loops survive for a few oscillation periods and we observe that their lifetime grows as  $L^2$ . We can explain this growth in terms of episodic particle radiation. When compared to gravitational energy losses, we find that gravitational radiation dominates for loops that are larger than a critical length (see Eq. (11)).

We thank the Lorentz Center for hosting the Topological Defects workshop where we had the opportunity to discuss these results with the participants, especially Jose Blanco-Pillado, Mark Hindmarsh, Ken Olum, Paul Shellard and Daniele Steer. DM and LP are supported in part by the National Sciences and Engineering Research Council (NSERC) of Canada. AS and TV are supported by the U.S. Department of Energy, Office of High Energy Physics, under Award No. DE-SC0018330

at Arizona State University. This research was enabled in part by support provided by WestGrid [27] and Compute Canada [28]. The bulk of the computations were performed on the Agave and Stampede2 clusters at Arizona State University and The University of Texas at Austin, respectively.

## Supplemental Material

In this Section, we describe the steps involved in setting up the initial configuration of fields in our simulation. First, we numerically find a solution for a static, infinite, straight string by substituting the Nielsen-Olesen ansatz (4) into the equations of motion and solving for the profile functions  $f(r)$  and  $v(r)$  using the relaxation method. We then use cubic spline interpolation to obtain smooth functions  $f(r)$  and  $v(r)$  and their derivatives.

To build a cosmic string loop we consider a string-antistring pair along the  $z$ -direction and another along the  $x$ -direction in a simulation box with periodic boundary conditions (PBC). We then Lorentz boost the strings and antistrings so that they are moving towards each other as shown in Fig. 1. Since the evolution equations (3) are in the temporal gauge, we must gauge transform the boosted string solutions to set the temporal component of the gauge field to zero. Namely, we find a gauge transform  $U = e^{ie\xi}$  such that

$$A_0 = \bar{A}_0 + \frac{i}{e}U\partial_t U^* = \bar{A}_0 + \partial_t \xi = 0, \quad (12)$$

$$A_i = \bar{A}_i + \frac{i}{e}U\partial_i U^* = \bar{A}_i + \partial_i \xi, \quad (13)$$

where  $A_\mu$  is in the temporal gauge and  $\bar{A}_\mu$  is the field after the Lorentz boost.

From (12), we have  $\partial_t \xi = -\bar{A}_0$  and  $\xi$  can be evaluated as

$$\xi = \int_0^t d\tau \bar{A}_0. \quad (14)$$

At initial time  $t = 0$ , this gives  $\xi = 0$ . Similarly  $\partial_i \xi|_{t=0} = 0$ . Hence, at the initial time, we have

$$A_0 = 0, \quad (15)$$

$$A_i = \bar{A}_i + \partial_i \xi|_{t=0} = \bar{A}_i, \quad (16)$$

where all functions are evaluated at  $t = 0$ . Note that the initial value of the scalar field is unaffected by the gauge transformation since  $\exp(ie\xi) = 1$  when  $\xi = 0$ .

To solve the equations of motion we also need  $\partial_t A_\mu$  and  $\partial_t \phi$  at the initial time. We have

$$\partial_t A_\mu|_{t=0} = \partial_t \bar{A}_\mu + \partial_t \partial_\mu \xi = \partial_t \bar{A}_\mu - \partial_\mu \bar{A}_0 \quad (17)$$

$$\partial_t \phi|_{t=0} = \partial_t \bar{\phi} - ie\bar{A}_0 \bar{\phi}. \quad (18)$$

where all functions are evaluated at  $t = 0$ .

To combine the string and anti-string solutions, we take the ansatz given by [1]

$$\phi_{s\bar{s}} = \frac{\phi_s \phi_{\bar{s}}}{\eta} = \frac{|\phi_s| |\phi_{\bar{s}}|}{\eta} e^{i(\theta_s - \theta_{\bar{s}})}, \quad (19)$$

$$A_{s\bar{s}} = A_s - A_{\bar{s}}. \quad (20)$$

To be consistent with the PBC, the phase of  $\phi_{s\bar{s}}$  must approach zero at the boundaries of the box. While in (20) the phase approaches zero asymptotically at infinity, it does not do so in a finite simulation box. Thus, we modified the ansatz to make the phase approach zero faster:

$$\phi_{s\bar{s},\text{mod}} = \frac{|\phi_s| |\phi_{\bar{s}}|}{\eta} e^{i(\theta_s - \theta_{\bar{s}})[1 - \tanh(\omega(\rho - L/2))]/2},$$

where  $\omega$ , taken to be 0.5, is a parameter that determines how quickly the phase approaches to 0 at the boundaries, and  $L$  is the size of the box. Finally, the scalar and gauge fields of the two sets of a parallel string-antistring pair are given as

$$\phi = \frac{\phi_{s\bar{s},1} \phi_{s\bar{s},2}}{\eta}, \quad (21)$$

$$A = A_{s\bar{s},1} + A_{s\bar{s},2}, \quad (22)$$

where  $\phi_{s\bar{s},1}, A_{s\bar{s},1}$  and  $\phi_{s\bar{s},2}, A_{s\bar{s},2}$  are the scalar and gauge fields of the first and second string - anti-string pairs, respectively.

- 
- [1] A. Vilenkin and E. P. S. Shellard, *Cosmic Strings and Other Topological Defects* (Cambridge University Press, 2000), ISBN 9780521654760, URL <http://www.cambridge.org/mw/academic/subjects/physics/theoretical-physics-and-mathematical-physics/cosmic-strings-and-other-topological-defects?format=PB>.
- [2] B. Abbott et al. (LIGO Scientific, Virgo), Phys. Rev. **D97**, 102002 (2018), 1712.01168.
- [3] P. D. Lasky et al., Phys. Rev. **X6**, 011035 (2016), 1511.05994.

- [4] J. J. Blanco-Pillado, K. D. Olum, and X. Siemens, Phys. Lett. **B778**, 392 (2018), 1709.02434.
- [5] A. Albrecht and N. Turok, Phys. Rev. Lett. **54**, 1868 (1985).
- [6] D. P. Bennett and F. R. Bouchet, Phys. Rev. **D41**, 2408 (1990).
- [7] B. Allen and E. P. S. Shellard, Phys. Rev. Lett. **64**, 119 (1990).
- [8] J. J. Blanco-Pillado, K. D. Olum, and B. Shlaer, Phys. Rev. **D83**, 083514 (2011), 1101.5173.
- [9] L. Lorenz, C. Ringeval, and M. Sakellariadou, JCAP **1010**, 003 (2010), 1006.0931.
- [10] M. Hindmarsh, J. Lizarraga, J. Urrestilla, D. Daveerio, and M. Kunz, Phys. Rev. **D96**, 023525 (2017), 1703.06696.
- [11] T. Vachaspati, A. E. Everett, and A. Vilenkin, Phys. Rev. **D30**, 2046 (1984).
- [12] M. Srednicki and S. Theisen, Phys. Lett. **B189**, 397 (1987).
- [13] R. H. Brandenberger, Nucl. Phys. **B293**, 812 (1987).
- [14] K. D. Olum and J. J. Blanco-Pillado, Phys. Rev. **D60**, 023503 (1999), gr-qc/9812040.
- [15] K. D. Olum and J. J. Blanco-Pillado, Phys. Rev. Lett. **84**, 4288 (2000), astro-ph/9910354.
- [16] C. J. A. P. Martins, J. N. Moore, and E. P. S. Shellard, Phys. Rev. Lett. **92**, 251601 (2004), hep-ph/0310255.
- [17] M. Hindmarsh, S. Stuckey, and N. Bevis, Phys. Rev. **D79**, 123504 (2009), 0812.1929.
- [18] T. Vachaspati, Phys. Rev. Lett. **117**, 181601 (2016), 1607.07460.
- [19] H. B. Nielsen and P. Olesen, Nucl. Phys. **B61**, 45 (1973), [302(1973)].
- [20] E. B. Bogomolny, Sov. J. Nucl. Phys. **24**, 449 (1976), [Yad. Fiz.24,861(1976)].
- [21] M. K. Prasad and C. M. Sommerfield, Phys. Rev. Lett. **35**, 760 (1975).
- [22] S. A. Teukolsky, Phys. Rev. **D61**, 087501 (2000), gr-qc/9909026.
- [23] URL <https://ayushsaurabh.home.blog>.
- [24] T. Vachaspati and A. Vilenkin, Phys. Rev. **D31**, 3052 (1985).
- [25] D. Garfinkle and T. Vachaspati, Phys. Rev. **D36**, 2229 (1987).
- [26] P. Binetruy, A. Bohe, T. Hertog, and D. A. Steer, Phys. Rev. **D80**, 123510 (2009), 0907.4522.
- [27] URL <http://www.westgrid.ca>.
- [28] URL <http://www.computecanada.ca>.